Clim. Past Discuss., 10, 3585–3616, 2014
www.clim-past-discuss.net/10/3585/2014/
doi:10.5194/cpd-10-3585-2014

Climate of the Past Discussions
Open Access

Optimisation of glaciological parameters for ice core chronology by implementing counted layers between identified depth levels

L. Bazin[1], B. Lemieux-Dudon[2], A. Landais[1], M. Guillevic[1,3], P. Kindler[4], F. Parrenin[5], and P. Martinerie[5]

[1]Laboratoire des Sciences du Climat et de l'Environnement, UMR8212, CEA–CNRS–UVSQ, Orme des Merisiers, Gif sur Yvette, France
[2]Laboratoire Jean Kuntzmann, Grenoble, France
[3]Centre for Ice and Climate, Niels Bohr Institute, University of Copenhagen, Copenhagen, Denmark
[4]Climate and Environmental Physics, Physics Institute & Oeschger Center for Climate Change Research, University of Bern, Bern, Switzerland
[5]Laboratoire de Glaciologie et Géophysique de l'Environnement, UMR 5183, Univ. Grenoble Alpes–CNRS, Grenoble, France

Received: 22 July 2014 – Accepted: 5 August 2014 – Published: 28 August 2014

Correspondence to: L. Bazin (lucie.bazin@lsce.ipsl.fr)

Published by Copernicus Publications on behalf of the European Geosciences Union.

CPD
10, 3585–3616, 2014

Abstract

A recent coherent chronology has been built for 4 Antarctic ice cores and the North-GRIP (NGRIP) Greenland ice core (Antarctic Ice Core Chronology 2012, AICC2012) using a bayesian approach for ice core dating (Datice). When building the AICC2012 chronology, and in order to prevent any confusion with official ice cores chronology, it has been imposed that the AICC2012 chronology for NGRIP should respect exactly the GICC05 chronology based on layer counting. However, such a strong tuning did not satisfy the hypothesis of independence of background parameters and observations for the NGRIP core as required by Datice. We present here the implementation in Datice of a new type of markers that is better suited to constraints deduced from layer counting: the markers of age-difference. Using this type of markers for NGRIP in a 5 cores dating exercise with Datice, we have performed several sensitivity tests and show that the new ice core chronologies obtained with these new markers do not differ by more than 400 years from AICC2012 for Antarctic ice cores and by more than 130 years from GICC05 for NGRIP over the last 60 000 years. With this new parameterization, the accumulation rate and lock-in depth associated with NGRIP are more coherent with independent estimates than those obtained in AICC2012. While these new chronologies should not be used yet as new ice core chronologies, the improved methodology presented here should be considered in the next coherent ice core dating exercise.

1 Introduction

The reference timescale for Greenland ice cores, GICC05, has been obtained by layer counting back to 60 ka (thousands of years before present, present being year 1950 all along our study; Vinther et al., 2006; Rasmussen et al., 2006; Andersen et al., 2006; Svensson et al., 2008). This chronology is absolute with an increasing associated uncertainty with depth, reaching more than 2.6 ka at 60 ka. Because this chronology is

CPD
10, 3585–3616, 2014

based on annual layer counting, the duration of events is rather precise, even for old ages, with an uncertainty of about 1–8 years for counting of 20 annual layers. Since the layer counting is not independent from one interval to another, the final uncertainty on the GICC05 chronology cumulates the counting error: uncertain annual layers are counted 0.5 ± 0.5 years, while certain layers are counted as 1 ± 0 years (Rasmussen et al., 2006). The 1-sigma uncertainty of GICC05 is thus expressed as half the Maximum Counting Error (MCE; Rasmussen et al., 2006).

This chronology has been used as a reference for many records of the North Atlantic region (Austin et al., 2012; Walker et al., 2012; Austin and Hibbert, 2012; Davies et al., 2012; Blockley et al., 2012b). It has also been used as a basis over the last 60 ka for the recent construction of the coherent Antarctic Ice Core Chronology (AICC2012) gathering one Greenland ice core (NorthGRIP – NGRIP) and 4 Antarctic ice cores (EPICA Dome C – EDC, EPICA Dronning Maud Land – EDML, Talos Dome ice core – TALDICE and Vostok) (Bazin et al., 2013; Veres et al., 2013). For the construction of AICC2012 with the bayesian tool Datice (Lemieux-Dudon et al., 2010), we have imposed a 1-sigma deviation for NGRIP of 50 years maximum. Even if such a constraint is artificially too strong compared to the true uncertainty of GICC05, it permits to keep a coherency within 5 years between the NGRIP AICC2012 chronology and GICC05.

Still, the strong tie of AICC2012 to GICC05 had raised some technical problems when optimizing the chronology with the bayesian tool Datice. Three glaciological parameters are indeed optimized during this process: accumulation rate, ice thinning and lock-in depth (i.e. the depth at which air is trapped when snow is sufficiently compacted). The bayesian approach imposes to start with first guess (background) scenarios for the three parameters. They are then modified within their imposed variance range so that the final chronology fits the absolute and relative age constraints for each ice core within error bars.

In practice, to force the NGRIP AICC2012 chronology to fit the GICC05 age scale, we had to use the modelled thinning function and accumulation rate adapted to the GICC05 chronology (hereafter DJ–GICC05 scenarios; Vinther et al., 2006; Rasmussen

CPD
10, 3585–3616, 2014

et al., 2006; Andersen et al., 2006; Svensson et al., 2008) as background thinning and accumulation rate scenarios in Datice. The associated variances were also imposed to be very small to prevent any deviation from the GICC05 timescale as well as absolute markers every 60 years with an artificial maximum uncertainty of 50 years for the NGRIP ice core.

Even if the uncertainty of the GICC05 timescale is well constrained, this is not true for the DJ–GICC05 scenarios of thinning and accumulation. The thinning function is deduced from a simple Dansgaard–Johnsen (DJ) ice flow model (Dansgaard and Johnsen, 1969; Andersen et al., 2006) that has been parameterized to obtain the best match between the modelled and observed depth–age horizons in the ice cores. Then, the thinning function calculated with the DJ model is used together with the observed annual layer thicknesses to produce an accumulation rate history. No uncertainty value is associated with the reconstructions of thinning and accumulation rate in Greenland ice cores but thinning reconstructed from such 1-D ice flow model are generally associated with an uncertainty of 30 % (Cutler et al., 1995).

Recently, studies combining air isotopic measurements (δ^{15}N of N_2) with firnification models have suggested that, both in NGRIP and NEEM, the accumulation rates reconstructed from the GICC05 or ss09sea chronologies, through layer counting and the DJ flow model, were overestimated during the last glacial period (Huber et al., 2006; Guillevic et al., 2013; Kindler et al., 2014). Indeed, δ^{15}N of N_2 of air trapped in an ice core indicates the depth and the amplitude of abrupt temperature changes in the gas phase through thermal fractionation. The depth difference between the same abrupt temperature changes recorded in the ice phase through ice δ^{18}O increase/decrease and in the gas phase through a positive/negative δ^{15}N peak is called delta–depth (Δdepth). Moreover, in the absence of any abrupt temperature change and convection at the top of the firn, the δ^{15}N gives an indication of the past lock-in depth (LID) due to gravitational fractionation. A firnification model including heat diffusion and mainly driven by temperature and accumulation rate can reproduce long term and abrupt δ^{15}N variations with depth for Greenland ice cores. Still, it has been shown that the δ^{15}N profile

CPD
10, 3585–3616, 2014

is best reproduced when the ss09sea accumulation rate for NGRIP is decreased by ∼ 20 % over the period 20 to 60 ka (Kindler et al., 2014; Huber et al., 2006).

It thus appears that the way NGRIP was implemented in the Datice tool for the AICC2012 chronology is not optimal. In addition to GICC05 chronological uncertainties that were not taken into account by construction, imposing the DJ-GICC05 accumulation rate and thinning scenarios with artificially reduced variances most probably led to incorrect output scenarios for these glaciological parameters.

In this paper, we propose an improvement of Datice to better implement the chronological uncertainties. We incorporate the possibility of integrating markers of age-difference and corresponding uncertainties instead of only absolute ages with artificially small uncertainties. This better respects the construction of the layer counted GICC05 chronology where the uncertainty on age differences is much smaller than on absolute ages. We also relax the strong constraints on thinning and accumulation rate and allow the NGRIP chronology to differ from GICC05 chronology within its error bars.

The outline of the manuscript is the following. In a first methodological section, we present the improvement made on the Datice tool in order to integrate the markers of age-difference with their uncertainties. Then, we show that the relaxation of the constraints on glaciological parameters enables removing some inconsistencies observed in the AICC2012 timescale. Finally, we focus on how this new version of Datice modifies the NGRIP and Antarctic chronologies compared to AICC2012.

2 Construction of the GICC05-free chronology

2.1 Methodology

The purpose of the following section is to describe the modifications implemented in Datice (Lemieux-Dudon et al., 2009, 2010) to take into account an additional type of constraint: the markers of age-difference. This constraint is applied by feeding Datice with the beginning and end depths of the interval, its duration and the duration uncer-

CPD
10, 3585–3616, 2014

tainty. A last parameter permits to correlate or not this uncertainty with other duration uncertainties at various depth levels. The main modification of the Datice code appears in the expression of the cost function. The minimization of the Datice cost function aims at obtaining the best age model scenario by taking into account the paleo–observations and a background (first guess) age model. The background age model and paleo–observations should be independent from each other. The minimization of the cost function permits to make the best compromise between independent information.

In practice, Datice is applied to N ice cores to calculate coherent chronologies for both the ice and gas phases. For the ice core indexed k, gas and ice chronologies are deduced from the scenarios of the three glaciological parameters optimized in Datice: the total thinning function $T_k(z)$, the accumulation rate $A_k(z)$ and the lock-in depth in ice equivalent (LIDIE) $C_k(z)$ (Appendix A). On the basis of these 3 key parameters, Datice defines the model scenario $\boldsymbol{X}$ as a set of correction functions $\alpha_k(z)$, $\tau_k(z)$ and $\gamma_k(z)$ to be applied as multiplicative factors on prior scenarios for the accumulation, thinning function and LIDIE respectively, for the core k and at each depth level:

$$T_k(z) = \tau_k(z) \cdot T_k^{\mathrm{b}}(z) \quad (1)$$

$$A_k(z) = \alpha_k(z) \cdot A_k^{\mathrm{b}}(z) \quad (2)$$

$$C_k(z) = \gamma_k(z) \cdot C_k^{\mathrm{b}}(z) \quad (3)$$

where the prior (or background) scenarios for the thinning, accumulation and LIDIE are referred to as $T_k^{\mathrm{b}}(z)$, $A_k^{\mathrm{b}}(z)$ and $C_k^{\mathrm{b}}(z)$. In order to run a Datice simulation, background scenarios as well as observations with their respective uncertainties must be provided. Note that a change of variable is applied to all parameters, $\tilde{x} = \log(x)$, since Datice makes the hypothesis of lognormally distributed errors for the background model scenarios $T_k^{\mathrm{b}}(z)$, $A_k^{\mathrm{b}}(z)$ and $C_k^{\mathrm{b}}(z)$. This change of variable enables to transform lognormal into normal probability density functions in the Bayes' theorem (Tarantola, 2005).

Until now, observation $\boldsymbol{Y}$ could be of the following types: ice and gas age markers ($^{\mathrm{ia}}$ and $^{\mathrm{ga}}$), delta-depth markers ($^{\mathrm{dd}}$), or ice and gas stratigraphic links ($^{\mathrm{is}}$ and $^{\mathrm{gs}}$) (Lemieux-

CPD
10, 3585–3616, 2014

Dudon et al., 2010; Buiron et al., 2011; Veres et al., 2013; Bazin et al., 2013). The application of a supplementary type of observation, named the markers of age-difference (^{ad}), leads to an additional term in the cost function (Eq. 4). This supplementary term (last term in Eq. 4) is added in the original cost function, under the hypothesis of no error correlation between (i) observations of different types, (ii) observation of different cores, or (iii) observation and background model scenarios.

$$
\begin{aligned}
J(\tilde{\boldsymbol{X}}) = & \sum_{k=1}^{N} \frac{1}{2} \left(\tilde{\boldsymbol{X}}_k - \tilde{\boldsymbol{X}}_k^{\mathrm{b}}\right)^T [\mathbf{B}]^{-1} \left(\tilde{\boldsymbol{X}}_k - \tilde{\boldsymbol{X}}_k^{\mathrm{b}}\right) \\
& + \sum_{k=1}^{N} \frac{1}{2} \left(\boldsymbol{Y}_k^{\mathrm{dd}} - \mathbf{h}_k^{\mathrm{dd}}(\tilde{\boldsymbol{X}}_k)\right)^T \left[\mathbf{R}_k^{\mathrm{dd}}\right]^{-1} \left(\boldsymbol{Y}_k^{\mathrm{dd}} - \mathbf{h}_k^{\mathrm{dd}}(\tilde{\boldsymbol{X}}_k)\right) \\
& + \sum_{k=1}^{N} \frac{1}{2} \left(\boldsymbol{Y}_k^{\mathrm{ia}} - \mathbf{h}_k^{\mathrm{ia}}(\tilde{\boldsymbol{X}}_k)\right)^T \left[\mathbf{R}_k^{\mathrm{ia}}\right]^{-1} \left(\boldsymbol{Y}_k^{\mathrm{ia}} - \mathbf{h}_k^{\mathrm{ia}}(\tilde{\boldsymbol{X}}_k)\right) \\
& + \sum_{k=1}^{N} \frac{1}{2} \left(\boldsymbol{Y}_k^{\mathrm{ga}} - \mathbf{h}_k^{\mathrm{ga}}(\tilde{\boldsymbol{X}}_k)\right)^T \left[\mathbf{R}_k^{\mathrm{ga}}\right]^{-1} \left(\boldsymbol{Y}_k^{\mathrm{ga}} - \mathbf{h}_k^{\mathrm{ga}}(\tilde{\boldsymbol{X}}_k)\right) \\
& + \sum_{k=1}^{N} \frac{1}{2} \left(\boldsymbol{Y}_k^{\mathrm{is}} - \mathbf{h}_k^{\mathrm{is}}(\tilde{\boldsymbol{X}}_k)\right)^T \left[\mathbf{R}_k^{\mathrm{is}}\right]^{-1} \left(\boldsymbol{Y}_k^{\mathrm{is}} - \mathbf{h}_k^{\mathrm{is}}(\tilde{\boldsymbol{X}}_k)\right) \\
& + \sum_{k=1}^{N} \frac{1}{2} \left(\boldsymbol{Y}_k^{\mathrm{gs}} - \mathbf{h}_k^{\mathrm{gs}}(\tilde{\boldsymbol{X}}_k)\right)^T \left[\mathbf{R}_k^{\mathrm{gs}}\right]^{-1} \left(\boldsymbol{Y}_k^{\mathrm{gs}} - \mathbf{h}_k^{\mathrm{gs}}(\tilde{\boldsymbol{X}}_k)\right) \\
& + \sum_{k=1}^{N} \frac{1}{2} \left(\boldsymbol{Y}_k^{\mathrm{ad}} - \mathbf{h}_k^{\mathrm{ad}}(\tilde{\boldsymbol{X}}_k)\right)^T \left[\mathbf{R}_k^{\mathrm{ad}}\right]^{-1} \left(\boldsymbol{Y}_k^{\mathrm{ad}} - \mathbf{h}_k^{\mathrm{ad}}(\tilde{\boldsymbol{X}}_k)\right) \qquad (4)
\end{aligned}
$$

In Eq. (4), the first term is related to the background term, while the six following terms are related to the observations. The cost function measures the squared distance

CPD
10, 3585–3616, 2014

between the background scenarios or observations with the current age model $\tilde{\boldsymbol{X}}$. The observation operators, **h**, have to be introduced to translate the observation value on the current age model at each iteration. All the squared distances are weighted according to the confidence we have in the background model scenarios and in the markers. This is done through the background error covariance matrix **B**, and the observation error covariance matrices **R**. These matrices play a key role since the weights they introduce set the final trade-off between the background and observation constraints in the cost function.

For NGRIP, indexed with k, each marker of age-difference is defined over a depth interval between $z_k^{\mathrm{ad},1}$ and $z_k^{\mathrm{ad},2}$. Such a marker measures the number of years y_k^{ad} counted in between the two depth levels.

Figure 1 shows the result of one Datice simulation, with the optimized ice chronology $\Psi_k^{\mathrm{a}}(z)$ (red line), and the background chronology (grey dotted line). Each marker of age-difference is sketched with a grey rectangle designed to confirm whether the analysed chronology meets the marker constraint or not:

$$\Psi_k^{\mathrm{a}}\left(z_k^{\mathrm{ad},2}\right) - \Psi_k^{\mathrm{a}}\left(z_k^{\mathrm{ad},1}\right) \leq y_k^{\mathrm{ad}} \pm \sigma_k^{\mathrm{ad}} \tag{5}$$

where $\Psi_k^{\mathrm{a}}\left(z_k^{\mathrm{ad},1}\right)$ and $\Psi_k^{\mathrm{a}}\left(z_k^{\mathrm{ad},2}\right)$ are the analysed ice ages at both ends of the depth interval over which $y_k^{\mathrm{ad}} \pm \sigma_k^{\mathrm{ad}}$ years were counted. The analysed ice age curve should therefore be located within the error bars close to the upper right corner of the rectangle.

2.2 Modifications of inputs since AICC2012

An important condition to use Datice properly is to respect the independence between the age constraints and the background scenarios. This was not the case when building AICC2012 for the NGRIP ice core. Here, the new development of Datice allows one to use scenarios for background accumulation rate and thinning function indepen-

CPD
10, 3585–3616, 2014

dent from the age constraints deduced from GICC05 for NGRIP. The thinning function is the same as for AICC2012, obtained from the 1-D–DJ glaciological model adapted to NGRIP (Andersen et al., 2006). However, we have largely increased its associated variance to make it comparable to the ones associated with the background thinning function of the other cores implemented in Datice (Appendix A). For the accumulation rate, we use two background scenarios independent from GICC05, i.e. based on variations of water isotopes or $\delta^{15}N$ of N_2 as detailed in Sect. 3.1. The formulation and coefficients of the variance of NGRIP background accumulation rate are the same as in AICC2012 and comparable to other ice cores. The LIDIE background scenario in AICC2012 was built from a firnification model (Goujon et al., 2003) whose input parameters (temperature and accumulation rate) were roughly adjusted to be coherent with the mean $\delta^{15}N$ values measured over the NGRIP ice core. It was thus independent from GICC05 and has been kept unchanged for our study.

Concerning the age constraint, the absolute age markers deduced from GICC05 were replaced by markers of age-difference. The markers of age-difference are obtained from the GICC05 chronology at regular time intervals. In the official GICC05 chronology, the markers of age-difference are given every 20 years with the corresponding Maximum Counting Error (MCE), but some adjustments of the periodicity of these age markers were done for this study (Sect. 2.3). In order to constrain the relative gas chronology vs the ice chronology, we use information derived from $\delta^{15}N$ of air trapped in ice bubbles. New $\delta^{15}N$ data on the NGRIP ice core have been published since the AICC2012 chronology (Kindler et al., 2014). In particular, these data permit to identify depths of rapid temperature increases associated with the beginning of Greenland Interstadials (GI) 1 to 7 in the gas phase. The depth differences between peaks of $\delta^{18}O_{ice}$ and $\delta^{15}N$ of a concomitant event recorded in the ice and the gas phases are thus used as delta-depth (Δdepth) constraints. With the new set of data from Kindler et al. (2014), we were thus able to deduce new Δdepth markers that were not available for the construction of AICC2012 (Table 1). Their uncertainties depend on the resolution of measurements and the difference of Δdepth estimates.

CPD
10, 3585–3616, 2014

2.3 Incorporation of the markers of age-difference in Datice

The introduction of the markers of age-difference is more appropriate to build a chronology the respecting the original layer counting constraints of the GICC05 chronology. Still, the incorporation of the GICC05 markers of age-difference and associated uncertainties within Datice is not straightforward. The main problems to address are (1) to define the most appropriate time interval for incorporation of the markers of age-difference and (2) to transform an uncertainty expressed as a maximum counting error in GICC05 into an uncertainty expressed as the standard deviation of a Gaussian distribution in Datice.

Different tests, summarized below, were performed to address these two problems and find the best formulation. To address the first problem of the periodicity of age markers, we have initially assumed that the MCE on each interval is completely uncorrelated over the last 60 ka and assigned a 2 MCE uncertainty to markers of age-difference deduced from the GICC05 layer counting. We decide in this paper to treat the error on individual annual layer as normally distributed. On this assumption, one can apply the MCE to age-difference markers as a Gaussian error. The periodicity of markers of age-difference in GICC05 is 20 years with a 1 to 8 years associated uncertainty (Rasmussen et al., 2006). However, as the spatial resolution of Datice is every meter, a too high frequency of the markers of age-difference can create inconsistencies. In particular, 1 m often represents more than 20 years for the NGRIP ice core over the last glacial period. As a consequence, even with an associated interpolation scheme, it is not possible for Datice to properly incorporate these markers and combine them with other dating constraints. This is illustrated on Fig. 2 where we have tested several intervals for the age-difference markers (20, 60, 100 and 200 years) with their corresponding 2 MCE errors. It resulted that markers have to be of 100 years difference or higher for Datice to run correctly without divergence at high depths. We then observe a difference of up to 130 years with the GICC05 chronology between 23–40 ka. We have chosen to retain the chronology built with markers of age-difference

CPD
10, 3585–3616, 2014

every 100 years in order to keep the strongest possible constraint from the GICC05 chronology.

In this first set of tests, the errors for markers of age-difference were assumed to be completely uncorrelated. This is the reason why even if we have chosen a larger uncertainty than the GICC05 one, the previous chronologies present final uncertainties 4 to 12 times smaller than the half MCE (Fig. 2 bottom). The assumption of uncorrelated errors for markers of age-difference is questionable since the layer counting process may introduce a systematic bias all over the core, or at least on several core sections. The MCE construction takes into account the possible existence of such error correlations by assuming completely correlated errors on individual annual layers. It gives an upper estimate of the error by summing up errors instead of squared errors (and taking the square root of the result). However, no estimate of the error correlation is provided in the GICC05 chronology. In order to test the influence of error correlation between markers of age-difference in our study, we have performed Datice simulations with different values of error correlation between markers of age-difference. For these tests, we have used a 100 years interval between markers of age-difference. We have assigned the value of 1 MCE for the 1-sigma uncertainty of Datice and the error correlation value has been varied between its minimum and maximum possible values. The introduction of the error correlation for markers of age-difference does not lead to strong deviations from the GICC05 chronology. As for the chronology built without correlation, the maximum difference between the new chronologies and GICC05 is of 130 years (Fig. 3). However, the chronologies obtained with or without correlation between errors are not similar: the deviation from GICC05 continuously increases with depth in the case of error correlation while the deviation is maximum for the last glacial maximum and then decreases in the case of no correlation. As expected, when the correlation is increased, the deviation between the new chronology and the first guess increases (Fig. 3 middle).

Even if the deviations from the GICC05 chronology are of the same order of magnitude with or without error correlation, the main difference appears in the final chronol-

CPD
10, 3585–3616, 2014

ogy uncertainty calculated by Datice (Fig. 3 bottom). Without error correlation, the 1-sigma uncertainty is close to 200 years at 60 ka compared to the double when we consider the error correlation for the markers of age difference. Still, the final error is smaller than the error given for the GICC05 chronology and defined as half the MCE. This result is not unexpected for two reasons. First, there is no direct link between half the MCE and a 1-sigma Gaussian error, even if both errors are symmetric. Second, the 1-sigma uncertainty obtained with Datice is the result of the chronology optimisation for 5 ice cores with many observations. For each depth level, the final uncertainty is then constrained by more precise sources of information than the age-difference markers. This may lead to a smaller final uncertainty than the one obtained with only one ice core and one kind of dating constraints.

Finally, we have tested several values of the correlation between errors within the possible range from 0 (no correlation) to 1 (complete correlation). Note that because of numerical problems linked to matrix inversion, values higher than 0.6 for error correlation led to improper runs of Datice for a 5 core exercise. Still, we have observed that the resulting chronologies showed only very small differences when varying the values of error correlation and especially the uncertainty on the final chronology does not increase significantly for error correlation higher than 0.3 (Fig. 3). This is due to the fact that the final Datice uncertainty does not depend only on the error on the age-difference markers but also on other markers uncertainties and background parameters covariances. In the following sections, we have first imposed the 2 MCE uncertainty and no error correlation; then we present the Datice results for the 0.5 error correlation simulation as comparison/confirmation of the changes compared to AICC2012 (dotted line on figures).

3 Glaciological implications

When we relax the constraints on the background glaciological parameters at NGRIP, Datice produces new optimized profiles for accumulation rate, thinning function and

CPD
10, 3585–3616, 2014

LIDIE. Because we work on a multi-site frame, the optimization takes into account not only the age-difference constraints from GICC05 but also the influence of the four Antarctic ice core chronologies through stratigraphic links.

3.1 Accumulation rate

Different background accumulation rate scenarios are tested for NGRIP. Two scenarios, independent from the GICC05 chronology, have been chosen. First, we use the accumulation associated with the ss09sea chronology (Johnsen et al., 2001). An accumulation rate scenario is deduced from the water isotope profile corrected for the isotopic composition of seawater, as it was done for Vostok, EDC, EDML and TALDICE (e.g. Lorius et al., 1985; Parrenin et al., 2007; Bazin et al., 2013). Then, the relationship between the accumulation rate and the $\delta^{18}O$ profile is adjusted in order for the 1-D–DJ ice flow model to match observed depth–age horizons. The obtained accumulation rate profile (ss09sea, Fig. 4) is fairly close to the DJ–GICC05 accumulation rate scenario over the millennial scale variability of the last glacial period. Nevertheless, the ss09sea accumulation rate is higher by $\sim 20\,\%$ than the DJ–GICC05 one at the end of the Younger Dryas and over the early Holocene. Alternatively, we have used the accumulation rate produced by Kindler et al. (2014), hereafter PK2014. It has been derived from ss09sea and adjusted with a firnification model (Schwander et al., 1997) to reproduce the $\delta^{15}N$ data measured over the glacial period. The PK2014 accumulation rate is much lower than the DJ–GICC05 accumulation rate over the last glacial period, by up to 30 %.

When taking ss09sea or PK2014 accumulation rate as background scenario and despite the difference between them, Datice produces very similar accumulation rates (Fig. 4). While the two output accumulation rate scenarios are much alike the DJ–GICC05 scenario over the early Holocene, they show significantly lower values than DJ–GICC05 for the last glacial period. On average, the Datice output accumulation rate for NGRIP is 10 to 15 % lower than the DJ–GICC05 accumulation rate over the

CPD
10, 3585–3616, 2014

glacial period after 60 ka. The same result is obtained for both the case with no error correlation and the case with error correlation (Fig. 4).

Our study confirms the overestimation of GICC05 accumulation rate already suggested by Guillevic et al. (2013) and Kindler et al. (2014), even if our accumulation rate scenarios for NGRIP are not showing values as low as those suggested by Kindler et al. (2014) on the δ^{15}N basis over the whole glacial period (Fig. 4). This conclusion is mainly valid for the last 60 ka since our study does not bring any improvement for the oldest part of NGRIP. For the following tests in this study, we chose to use the ss09sea accumulation rate as background.

3.2 Lock-in depth in ice equivalent

When building the AICC2012 chronology, we used a background LIDIE obtained from a densification model (Goujon et al., 2003). Indeed, in Greenland the LIDIE produced by the densification model is in agreement with the LIDIE deduced from δ^{15}N measurements (Huber et al., 2006; Guillevic et al., 2013). The background LIDIE scenario for NGRIP in AICC2012 was thus in agreement with the δ^{15}N mean level over the last 120 ka (Landais et al., 2004, 2005; Huber et al., 2006; Kindler et al., 2014). Still, because the δ^{15}N data from Kindler et al. (2014) were not published at that time, we could not implement the Δdepth constraints at the beginning of GI 1 to 7 as done here (Sect. 2.2).

When running Datice as for AICC2012, i.e. with the strong constraints to the GICC05 chronology, thinning function and accumulation rate for NGRIP, and with the addition of the new Δdepth constraints from Kindler et al. (2014), we obtain very large LIDIE levels for NGRIP between 28 and 38 ka (Fig. 5). LIDIE levels are deeper than 100 m, implying a lock-in depth exceeding 140 m. Deepest lock-in depths observed today in Antarctica are about 100–110 m deep (Landais et al., 2006) and NGRIP glacial lock-in depth is not expected to be deeper than 90 m from firnification models (Goujon et al., 2003). These large values were not obtained for AICC2012 in the absence of Δdepth constraints at the onset of GI 1 to 7. The Δdepth constraints from δ^{15}N measurements

CPD
10, 3585–3616, 2014

cannot be questioned since the δ^{15}N peaks in Greenland air bubbles clearly respond to abrupt surface temperature increases and are thus in phase with the increases in water isotopes (δ^{18}O) recorded in the ice phase. On the opposite, the DJ–GICC05 thinning function is very smooth and could be revised to be more realistic and sensitive to changes in ice properties (Guillevic et al., 2013). Since the LIDIE is simply calculated as Δdepth divided by the thinning function, a too small thinning function will lead to a too high LIDIE.

In our study, the NGRIP thinning function is not tied to the DJ estimate as in AICC2012 and it deviates significantly during the glacial period. As a result, the output LIDIE is not showing very strong values exceeding 100 m, which is more realistic (light blue curve, Fig. 5). We still observe quite large variations of the LIDIE by more than 15 m between 1900 and 2100 m. These variations are much larger than the LIDIE variations deduced from δ^{15}N mean levels over this depth interval (brown curve, Fig. 5). Indeed, except during abrupt warming, the δ^{15}N level in air trapped in ice is only influenced by gravitational fractionation (Severinghaus et al., 1998). In the absence of a deep convective zone at the surface of the firn, the δ^{15}N level can thus be linked directly to the firn depth. To reduce the non realistic short-term variations of LIDIE, we have thus reduced the variance of the background LIDIE ($\sigma_{b,L}$ = 0.6 to 0.3 and minimum value at 0.05, Appendix A, pink curve Fig. 5). The final LIDIE is in better agreement with the one deduced from δ^{15}N measurements. Note that this modification of the LIDIE variance has only a very minor effect on the chronology, thinning function and accumulation rate. Again, both simulations with or without error correlation lead to nearly the same results (Fig. 5).

4 Chronological and climatic implications

As an introduction, we strengthen that the GICC05-free chronologies discussed here should not be taken as new official chronologies but rather as studies of glaciological and climatic implications of reducing some constraints in the chronology construction.

CPD
10, 3585–3616, 2014

The AICC2012 chronology has the strong advantage of being in exact agreement with the GICC05 chronology and hence to facilitate the multi-archives comparison taking GICC05 as reference as already made in many studies (INTIMATE project: Blockley et al., 2012a). When looking at the NGRIP ice records, the final GICC05-free chronologies do not differ from the GICC05 or AICC2012 chronologies by more than 130 years over the last 60 ka (Fig. 6).

The Antarctic chronologies are not much modified compared to the AICC2012 chronologies. Both EDML and EDC GICC05-free chronologies differ by less than 400 years from AICC2012 (Fig. 6), which is well within the uncertainties of these chronologies (400–1000 years over this period). The small differences between the new GICC05-free and AICC2012 chronologies mean that the relationship between Greenland and Antarctic climate discussed with AICC2012 for the millennial scale variability of the last glacial period stays valid on GICC05-free (Veres et al., 2013). We observe a classical seesaw pattern with Antarctic temperature increasing during the Greenland stadials, with a faster and shorter increase at EDML than at EDC (Fig. 7).

5 Conclusions

The bayesian tool Datice used for the construction of the AICC2012 chronology has been improved and now enables one to consider the duration of events as dating constraints. This development is more coherent with the building of chronologies based on layer counting where the absolute error, defined as the maximum counted error, increases with depth because of a cumulative effect. To account for the fact that the counted errors on each interval are not uncorrelated, we have also introduced a correlation between age-difference errors. This has permitted us to produce coherent Greenland–Antarctica timescales that respect the correlated counting errors of GICC05 without forcing artificially the glaciological background parameters. Compared to the AICC2012 results, the NGRIP glaciological parameters obtained in this study are in better agreement with expected behaviours: (1) the accumulation rate is decreased

CPD
10, 3585–3616, 2014

in agreement with independent studies based on δ^{15}N measurements; (2) the LIDIE is in agreement with typical firn depth expected in Greenland. The final chronology does not differ by more than 130 years from GICC05 for NGRIP, which is well within the published uncertainty. For Antarctic ice cores, no difference larger than 400 years is observed and the bipolar seesaw pattern is not modified with these new chronologies. As a consequence and to avoid confusion with the reference GICC05 timescale, we do not recommend to use GICC05-free chronologies. However, the improvements performed in this study should be incorporated in the next coherent ice core dating effort. A more specific study on the determination and variation of the error correlation of the layer counted GICC05 chronology, and its translation as age-difference markers in Datice should be performed in the future.

Appendix A: Ages calculation in Datice and background variances definitions

The Datice age models are derived from three key ice core quantities: the total thinning function ($T(z)$), the accumulation rate ($A(z)$) and the LIDIE ($C(z)$). They allow to estimate the ice age chronology ($\Psi(z)$) as follows:

$$\Psi(z) = \int_0^z \frac{D(z')}{T(z') \cdot A(z')} \mathrm{d}z' \quad \text{(A1)}$$

with $D(z)$ being the relative density of the snow/ice material. The gas chronology ($\chi(z)$), is calculated using Δdepth, which measures the in-situ depth difference between ice and gas of the same age. Then the gas age is defined as the ice age of the layer situated at the depth ($z - \Delta\text{depth}$).

$$\Delta\text{depth}(z) = C(z) \cdot T(z) \quad \text{(A2)}$$

$$\chi(z) = \Psi(z - \Delta\text{depth}(z)) \quad \text{(A3)}$$

CPD
10, 3585–3616, 2014

The background parameters with their associated variances, as well as age constraints and their respective uncertainties are needed to calculate the optimized ages. Depending of the confidence assigned to the background parameters, Datice will be authorized to correct them more or less. Here we remind the formulations used to define the thinning function (Eq. A4) and the LIDIE (Eq. A5) variances, as several coefficients were corrected in this study.

The standard deviation of the thinning function is defined as:

$$\sigma_T(z) = c_{T_1} + c_{T_2} \cdot \int^{z} \frac{D(z)}{T(z)} \mathrm{d}z + c_{T_3} \cdot \frac{\sigma_{A,\mathrm{loc}}}{\sigma_{A,\mathrm{loc}}^{\max}} \tag{A4}$$

where c_{T_1}, c_{T_2} and c_{T_3} are user defined constant parameters (c_{T_2} equals $c \cdot 0.1/H$ where H is the maximum depth of the input and c a user defined constant), $T(z)$ is the thinning function, $D(z)$ the relative density, $\sigma_{A,\mathrm{loc}}$ the local standard deviation of accumulation and $\sigma_{A,\mathrm{loc}}^{\max}$ the maximum standard deviation of accumulation. The last term was implemented in order to increase the thinning variance during large climatic transitions since it has been suggested that the mechanical properties of ice can be modified in these periods. For the purpose of the tests performed in this study, we have corrected the c_{T_2} value (from 0.000016 to 0.000064) that was used for NGRIP when building AICC2012. This correction permits to have a coherent parameterization of the thinning variance for the 5 ice cores. Moreover, we have reduced the c_{T_1} values from 0.01 to 0.00001 in order to be closer to the 0 variance hypothesis at the surface for all sites. The other coefficients have the same values as used to build AICC2012 (SOM Bazin et al., 2013).

The formulation for the LIDIE standard deviation is:

$$\sigma_L(z) = \frac{\sigma_{\mathrm{b,L}}}{\sigma_{\mathrm{b},A}} \cdot \frac{\sigma_A(z)}{1 + \frac{m_{A,\mathrm{loc}}}{m_{A,\mathrm{loc}}^{\max}}} \tag{A5}$$

CPD
10, 3585–3616, 2014

with $m_{A,\mathrm{loc}}$ being the local mean accumulation rate and $m^{\max}_{A,\mathrm{loc}}$ its maximum value over the length of the core, $\sigma_{\mathrm{b,L}}$ is a reference standard deviation. In this case, the variance on the LIDIE increases with the variance on the accumulation rate, i.e. with the deviation from present-day conditions. This is justified by the fact that we do not have a standardized way to link LIDIE to accumulation rate and/or temperature (firnification model or δ^{15}N based estimate). In Sect. 3.2 we have reduced the value of the $\sigma_{\mathrm{b,L}}$ coefficient from 0.6 to 0.3 as well as the minimum value possible (from 0.1 to 0.05) for NGRIP. This means that we have more confidence in our background LIDIE scenario than when building the AICC2012 chronology. The other coefficients have the same values as used to build AICC2012 (SOM Bazin et al., 2013).

Acknowledgements. We thank Eric Wolff for his comments on a preliminary version of this article. This project was funded by the "Fondation de France Ars Cuttoli". This work was supported by Labex L-IPSL which is funded by the ANR (Grant n°ANR-10-LABX-0018). This is LSCE contribution no XX.

References

Andersen, K. K., Svensson, A., Johnsen, S. J., Rasmussen, S. O., Bigler, M., Röthlisberger, R., Ruth, U., Siggaard-Andersen, M.-L., Peder Steffensen, J., Dahl-Jensen, D., Vinther, B. M., and Clausen, H. B.: The Greenland Ice Core Chronology 2005, 15 42 ka. Part 1: constructing the time scale, Quaternary Sci. Rev., 25, 3246–3257, doi:10.1016/j.quascirev.2006.08.002, 2006.

Austin, W. E. and Hibbert, F. D.: Tracing time in the ocean: a brief review of chronological constraints (60–8 kyr) on North Atlantic marine event-based stratigraphies, Quaternary Sci. Rev., 36, 28–37, doi:10.1016/j.quascirev.2012.01.015, 2012.

Austin, W., Hibbert, F., Rasmussen, S., Peters, C., Abbott, P., and Bryant, C.: The synchronization of palaeoclimatic events in the North Atlantic region during Greenland Stadial 3 (ca 27.5 to 23.3 kyr b2k), Quaternary Sci. Rev., 36, 154–163, doi:10.1016/j.quascirev.2010.12.014, 2012.

Bazin, L., Landais, A., Lemieux-Dudon, B., Toyé Mahamadou Kele, H., Veres, D., Parrenin, F., Martinerie, P., Ritz, C., Capron, E., Lipenkov, V., Loutre, M.-F., Raynaud, D., Vinther, B., Svensson, A., Rasmussen, S. O., Severi, M., Blunier, T., Leuenberger, M., Fischer, H., Masson-Delmotte, V., Chappellaz, J., and Wolff, E.: An optimized multi-proxy, multi-site Antarctic ice and gas orbital chronology (AICC2012): 120–800 ka, Clim. Past, 9, 1715–1731, doi:10.5194/cp-9-1715-2013, 2013.

Blockley, S., Lane, C., Turney, C., and Bronk Ramsey, C.: The INTegration of Ice core, MArine and TErrestrial records of the last termination (INTIMATE) 60 000 to 8000 BP, Quaternary Sci. Rev., 36, 2–10, doi:10.1016/j.quascirev.2011.10.001, 2012a.

Blockley, S. P., Lane, C. S., Hardiman, M., Rasmussen, S. O., Seierstad, I. K., Steffensen, J. P., Svensson, A., Lotter, A. F., Turney, C. S., and Bronk Ramsey, C.: Synchronisation of palaeoenvironmental records over the last 60,000 years, and an extended INTIMATE event stratigraphy to 48 000 b2k, Quaternary Sci. Rev., 36, 1, doi:10.1016/j.quascirev.2011.09.017, 2012b.

Buiron, D., Chappellaz, J., Stenni, B., Frezzotti, M., Baumgartner, M., Capron, E., Landais, A., Lemieux-Dudon, B., Masson-Delmotte, V., Montagnat, M., Parrenin, F., and Schilt, A.: TALDICE-1 age scale of the Talos Dome deep ice core, East Antarctica, Clim. Past, 7, 1–16, doi:10.5194/cp-7-1-2011, 2011.

Cutler, N. N., Raymond, C. F., Waddington, E. D., Meese, D. A., and Alley, R. B.: The effect of ice-sheet thickness change on the accumulation history inferred from GISP2 layer thicknesses, Ann. Glaciol., 21, 26–32, 1995.

Dansgaard, W. and Johnsen, S. J.: A flow model and a time scale for the ice core from Camp Century, Greenland, J. Glaciol., 8, 215–223, 1969.

Davies, S. M., Abbott, P. M., Pearce, N. J., Wastegard, S., and Blockley, S. P.: Integrating the INTIMATE records using tephrochronology: rising to the challenge, Quaternary Sci. Rev., 36, 11–27, doi:10.1016/j.quascirev.2011.04.005, 2012.

EPICA Community Members: One-to-one coupling of glacial climate variability in Greenland and Antarctica, Nature, 444, 195–198, doi:10.1038/nature05301, 2006.

EPICA Community Members: Stable oxygen isotopes of ice core EDML, PANGAEA, doi:10.1594/PANGAEA.754444, 2010.

Goujon, C., Barnola, J.-M., and Ritz, C.: Modeling the densification of polar firn including heat diffusion: application to close-off characteristics and gas isotopic fractionation for Antarc-

CPD
10, 3585–3616, 2014

tica and Greenland sites, J. Geophys. Res.-Atmos., 108, 4792, doi:10.1029/2002JD003319, 2003.
Guillevic, M., Bazin, L., Landais, A., Kindler, P., Orsi, A., Masson-Delmotte, V., Blunier, T., Buchardt, S. L., Capron, E., Leuenberger, M., Martinerie, P., Prié, F., and Vinther, B. M.: Spatial gradients of temperature, accumulation and δ^{18}O-ice in Greenland over a series of Dansgaard–Oeschger events, Clim. Past, 9, 1029–1051, doi:10.5194/cp-9-1029-2013, 2013.
Huber, C., Beyerle, U., Leuenberger, M., Schwander, J., Kipfer, R., Spahni, R., Severinghaus, J. P., and Weiler, K.: Evidence for molecular size dependent gas fractionation in firn air derived from noble gases, oxygen, and nitrogen measurements, Earth Planet. Sc. Lett., 243, 61–73, doi:10.1016/j.epsl.2005.12.036, 2006.
Johnsen, S. J., Dahl-Jensen, D., Gundestrup, N., Steffensen, J. P., Clausen, H. B., Miller, H., Masson-Delmotte, V., Sveinbjornsdottir, A. E., and White, J.: Oxygen isotope and palaeotemperature records from six Greenland ice-core stations: Camp Century, Dye-3, GRIP, GISP2, Renland and NorthGRIP, J. Quaternary Sci., 16, 299–307, doi:10.1002/jqs.622, 2001.
Jouzel, J., Masson-Delmotte, V., Cattani, O., Dreyfus, G., Falourd, S., Hoffmann, G., Minster, B., Nouet, J., Barnola, J. M., Chappellaz, J., Fischer, H., Gallet, J. C., Johnsen, S., Leuenberger, M., Loulergue, L., Luethi, D., Oerter, H., Parrenin, F., Raisbeck, G., Raynaud, D., Schilt, A., Schwander, J., Selmo, E., Souchez, R., Spahni, R., Stauffer, B., Steffensen, J. P., Stenni, B., Stocker, T. F., Tison, J. L., Werner, M., and Wolff, E. W.: Orbital and millennial Antarctic climate variability over the past 800 000 years, Science, 317, 793, doi:10.1126/science.1141038, 2007.
Kindler, P., Guillevic, M., Baumgartner, M., Schwander, J., Landais, A., and Leuenberger, M.: Temperature reconstruction from 10 to 120 kyr b2k from the NGRIP ice core, Clim. Past, 10, 887–902, doi:10.5194/cp-10-887-2014, 2014.
Landais, A., Barnola, J. M., Masson-Delmotte, V., Jouzel, J., Chappellaz, J., Caillon, N., Huber, C., Leuenberger, M., and Johnsen, S. J.: A continuous record of temperature evolution over a sequence of Dansgaard–Oeschger events during Marine Isotopic Stage 4 (76 to 62 kyr BP), Geophys. Res. Lett., 31, L22211, doi:10.1029/2004GL021193, 2004.
Landais, A., Jouzel, J., Masson-Delmotte, V., and Caillon, N.: Large temperature variations over rapid climatic events in Greenland: a method based on air isotopic measurements, C. R. Geosci., 337, 947–956, doi:10.1016/j.crte.2005.04.003, 2005.

CPD
10, 3585–3616, 2014

Landais, A., Waelbroeck, C., and Masson-Delmotte, V.: On the limits of Antarctic and marine climate records synchronization: lag estimates during marine isotopic stages 5d and 5c, Paleoceanography, 21, PA1001, doi:10.1029/2005PA001171, 2006.

Lemieux-Dudon, B., Parrenin, F., and Blayo, E.: A probabilistic method to construct an optimal ice chronology for ice cores, in: Hondoh, T., Proceedings of the 2nd International Workshop on Physics of Ice Core Records (PICR-2), Institute of Low Temperature Science, Hokkaido University, Sapporo, Japan, 2009.

Lemieux-Dudon, B., Blayo, E., Petit, J.-R., Waelbroeck, C., Svensson, A., Ritz, C., Barnola, J.-M., Narcisi, B. M., and Parrenin, F.: Consistent dating for Antarctic and Greenland ice cores, Quaternary Sci. Rev., 29, 8–20, doi:10.1016/j.quascirev.2009.11.010, 2010.

Lorius, C., Ritz, C., Jouzel, J., Merlivat, L., and Barkov, N. I.: A 150,000-year climatic record from Antarctic ice, Nature, 316, 591–596, doi:10.1038/316591a0, 1985.

NorthGRIP Community Members: High-resolution record of Northern Hemisphere climate extending into the last interglacial period, Nature, 431, 147–151, doi:10.1038/nature02805, 2004.

Parrenin, F., Barnola, J.-M., Beer, J., Blunier, T., Castellano, E., Chappellaz, J., Dreyfus, G., Fischer, H., Fujita, S., Jouzel, J., Kawamura, K., Lemieux-Dudon, B., Loulergue, L., Masson-Delmotte, V., Narcisi, B., Petit, J.-R., Raisbeck, G., Raynaud, D., Ruth, U., Schwander, J., Severi, M., Spahni, R., Steffensen, J. P., Svensson, A., Udisti, R., Waelbroeck, C., and Wolff, E.: The EDC3 chronology for the EPICA Dome C ice core, Clim. Past, 3, 485–497, doi:10.5194/cp-3-485-2007, 2007.

Rasmussen, S. O., Andersen, K. K., Svensson, A. M., Steffensen, J. P., Vinther, B. M., Clausen, H. B., Siggaard-Andersen, M.-L., Johnsen, S. J., Larsen, L. B., Dahl-Jensen, D., Bigler, M., Röthlisberger, R., Fischer, H., Goto-Azuma, K., Hansson, M. E., and Ruth, U.: A new Greenland ice core chronology for the last glacial termination, J. Geophys. Res.-Atmos., 111, D06102, doi:10.1029/2005JD006079, 2006.

Schwander, J., Sowers, T., Barnola, J.-M., Blunier, T., Fuchs, A., and Malaizé, B.: Age scale of the air in the summit ice: Implication for glacial-interglacial temperature change, J. Geophys. Res.-Atmos., 102, 19483–19493, doi:10.1029/97JD01309, 1997.

Severinghaus, J. P., Sowers, T., Brook, E. J., Alley, R. B., and Bender, M. L.: Timing of abrupt climate change at the end of the Younger Dryas interval from thermally fractionated gases in polar ice, Nature, 391, 141–146, doi:10.1038/34346, 1998.

CPD
10, 3585–3616, 2014

Svensson, A., Andersen, K. K., Bigler, M., Clausen, H. B., Dahl-Jensen, D., Davies, S. M., Johnsen, S. J., Muscheler, R., Parrenin, F., Rasmussen, S. O., Röthlisberger, R., Seierstad, I., Steffensen, J. P., and Vinther, B. M.: A 60 000 year Greenland stratigraphic ice core chronology, Clim. Past, 4, 47–57, doi:10.5194/cp-4-47-2008, 2008.

Tarantola, A.: Inverse Problem Theory and Methods for Model Parameter Estimation, Society for Industrial and Applied Mathematics, doi:10.1137/1.9780898717921, 2005.

Veres, D., Bazin, L., Landais, A., Toyé Mahamadou Kele, H., Lemieux-Dudon, B., Parrenin, F., Martinerie, P., Blayo, E., Blunier, T., Capron, E., Chappellaz, J., Rasmussen, S. O., Severi, M., Svensson, A., Vinther, B., and Wolff, E. W.: The Antarctic ice core chronology (AICC2012): an optimized multi-parameter and multi-site dating approach for the last 120 thousand years, Clim. Past, 9, 1733–1748, doi:10.5194/cp-9-1733-2013, 2013.

Vinther, B. M., Clausen, H. B., Johnsen, S. J., Rasmussen, S. O., Andersen, K. K., Buchardt, S. L., Dahl-Jensen, D., Seierstad, I. K., Siggaard-Andersen, M.-L., Steffensen, J. P., Svensson, A., Olsen, J., and Heinemeier, J.: A synchronized dating of three Greenland ice cores throughout the Holocene, J. Geophys. Res.-Atmos., 111, D13102, doi:10.1029/2005JD006921, 2006.

Walker, M., Lowe, J., Blockley, S. P., Bryant, C., Coombes, P., Davies, S., Hardiman, M., Turney, C. S., and Watson, J.: Late glacial and early Holocene palaeoenvironmental "events" in Sluggan Bog, Northern Ireland: comparisons with the Greenland NGRIP GICC05 event stratigraphy, Quaternary Sci. Rev., 36, 124–138, doi:10.1016/j.quascirev.2011.09.008, 2012.

CPD
10, 3585–3616, 2014

Table 1. New Δdepth markers of NGRIP deduced from the data of Kindler et al. (2014).

depth (m)	Δdepth (m)	σ (m)
1490.2	25.07	2.5
1520.5	21.84	2.5
1574.4	23.51	2.5
1603.0	26.42	2.5
1792.7	25.07	2.5
1868.1	22.62	2.5
1888.4	21.87	2.5
1950.6	21.32	2
1972.6	20.42	2
2007.8	19.22	2
2099.9	17.77	2

CPD
10, 3585–3616, 2014

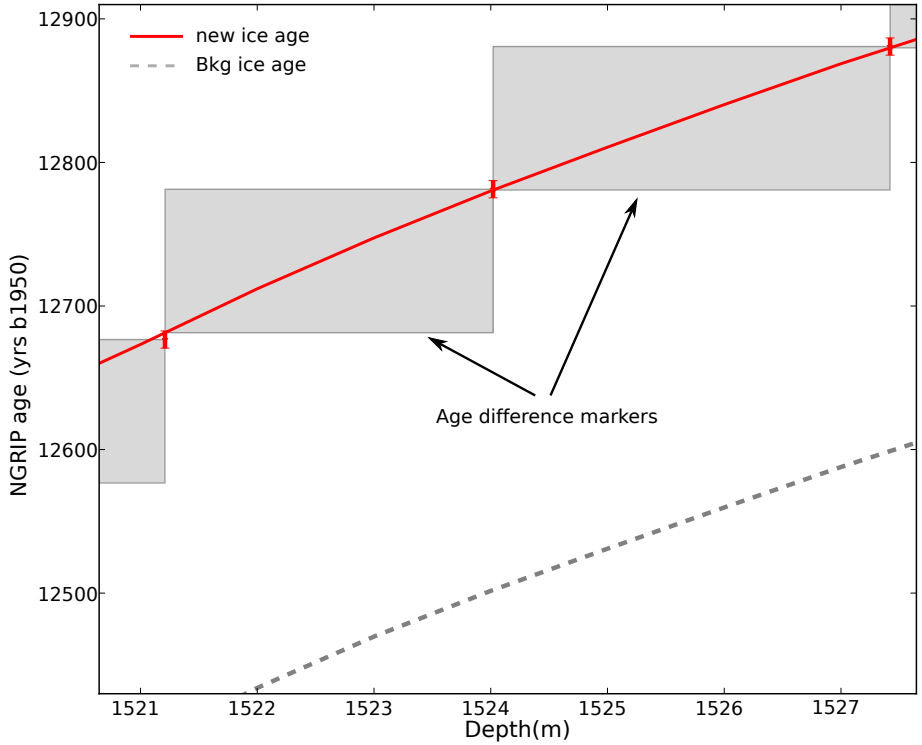

Figure 1. NGRIP ice chronologies centred on two markers of age-difference, over the depth interval 1521–1527 m. The red curve is the analysed ice chronology $\Psi_k^a(z)$, the grey dotted line is the background chronology. The grey rectangles represent the markers of age-difference. The lower left corner of the grey rectangle is attached to the analysed ice chronology, so that its abscissa and ordinate are $\left(z_k^{ad,1}, \Psi_k^a\left(z_k^{ad,1}\right)\right)$. The height of the rectangle equals the counted number of years y_k^{ad}, and the observation error bars $\pm\sigma_k^{ad}$ (red vertical bars) are centred on the upper right corner.

CPD
10, 3585–3616, 2014

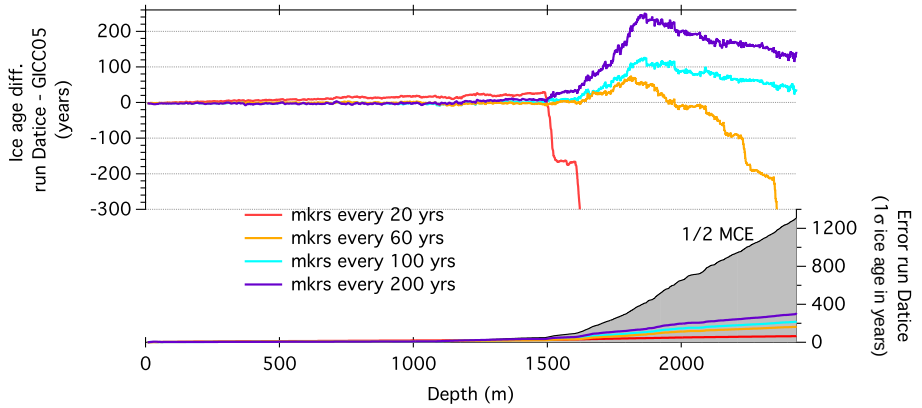

Figure 2. Comparison of age differences with GICC05 chronology for different intervals of age-difference markers over the period covered by layer counting. Top: the difference is calculated for markers every 20 years (red), every 60 years (orange), every 100 years (blue) and every 200 years (purple). Bottom: the corresponding colours represent the final uncertainties calculated by Datice for each frequency of markers. The 1-sigma uncertainty of GICC05 chronology is represented by the grey surface.

CPD
10, 3585–3616, 2014

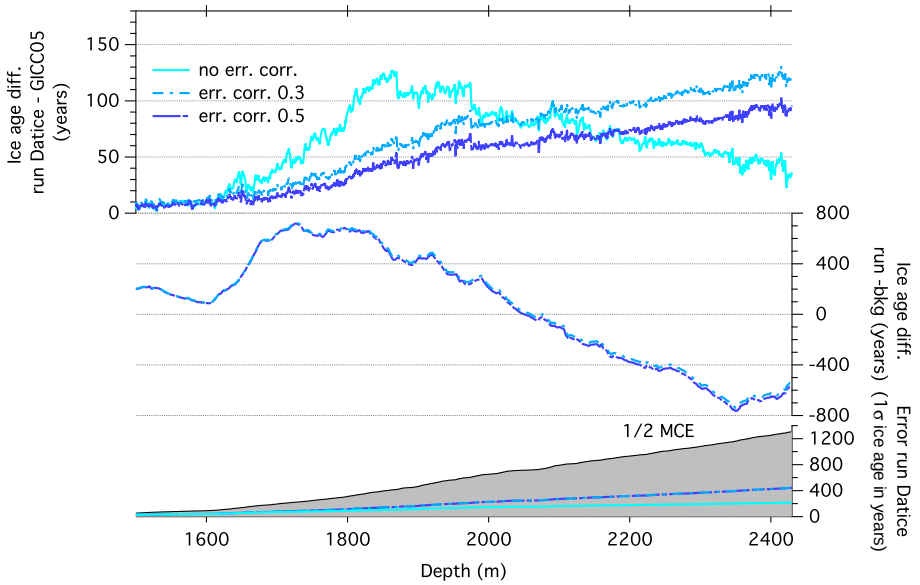

Figure 3. Top: comparison of age differences with GICC05 for Datice simulations when considering markers of age-difference without correlation (light blue line), with low correlation (dashed turquoise line) or moderate correlation (dark blue line). Middle: deviation of the new Datice chronologies from their background estimates for the two simulations considering error correlation. Bottom: 1-sigma error of NGRIP chronologies for GICC05 (grey surface), Datice without error correlation (light blue), with low error correlation (dashed turquoise line) or moderate error correlation (dark blue line) for the markers of age-difference.

CPD
10, 3585–3616, 2014

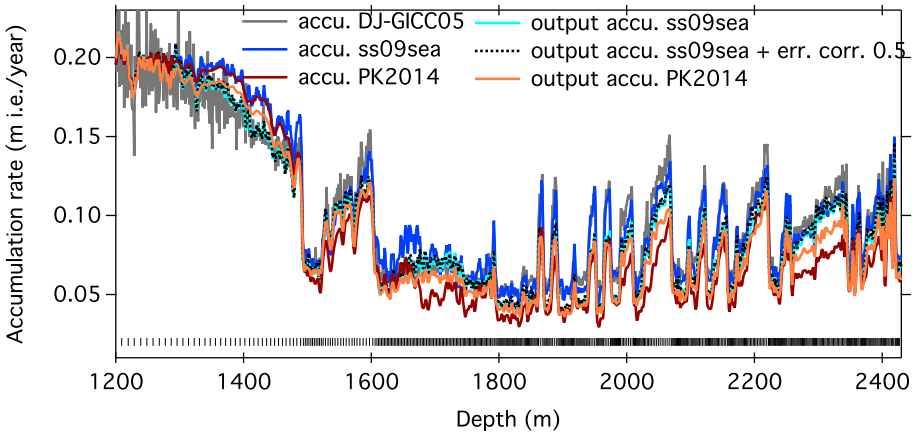

Figure 4. Comparison of accumulation rates for NGRIP over the last 60 ka. The GICC05 accumulation rate (grey) is presented for comparison; the ss09sea (dark blue) and PK2014 (brown) accumulation rates used as background; the Datice output accumulation rates using ss09sea (light blue for the run without error correlation, black dotted line for the run with error correlation) and PK2014 (orange) ones as input. The vertical bars at bottom indicate the positions of the markers of age-difference every 100 years.

CPD
10, 3585–3616, 2014

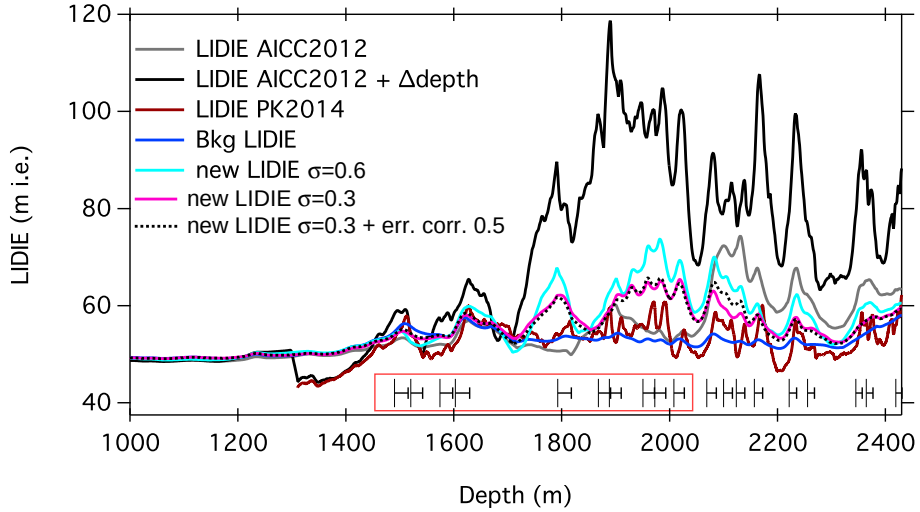

Figure 5. Comparison of NGRIP LIDIE over the glacial period. The LIDIE obtained when building the AICC2012 chronology (grey), the same as AICC2012 + Δdepth markers deduced from Kindler et al. (2014) (black) and the LIDIE obtained from the δ^{15}N data Kindler et al. (2014) are shown for comparison. The background LIDIE used as input is in dark blue. The output LIDIE after running Datice are also presented, in light blue when using the same error as in AICC2012 and in pink/black dotted line when reducing this error. The markers present at the bottom correspond to the Δdepth markers implemented in Datice. The ones in the red box are new Δdepth markers deduced from the data of Kindler et al. (2014).

CPD
10, 3585–3616, 2014

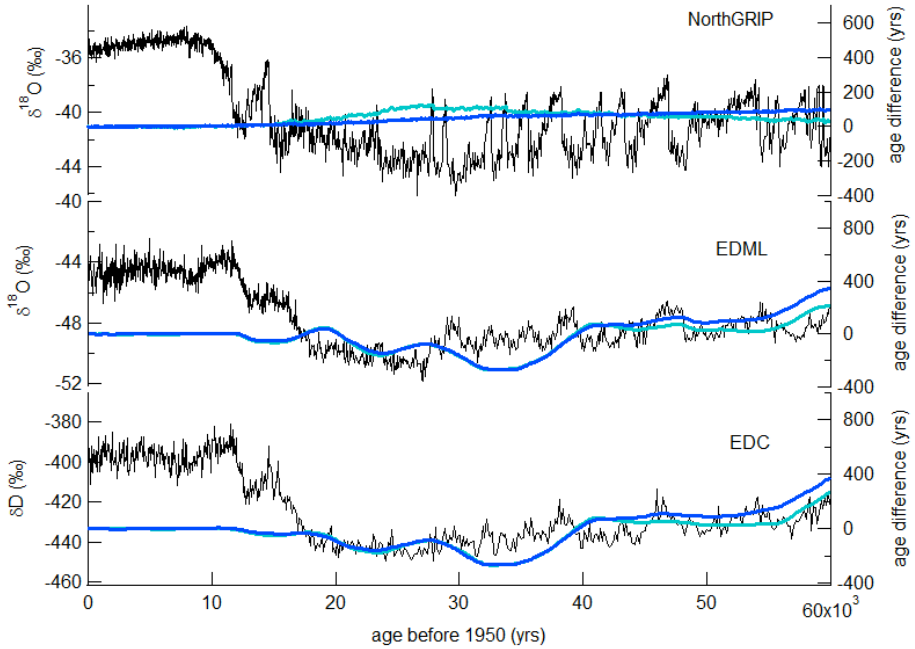

Figure 6. Water isotopic records (black) of NGRIP, EDML and EDC over the last 60 ka on the GICC05-free chronology without error correlation (NorthGRIP Community Members, 2004; EPICA Community Members, 2006, 2010; Jouzel et al., 2007). The blue solid lines indicate the age differences between the GICC05-free and the AICC2012 chronologies (dark blue: run with error correlation; light blue: run without error correlation).

CPD
10, 3585–3616, 2014

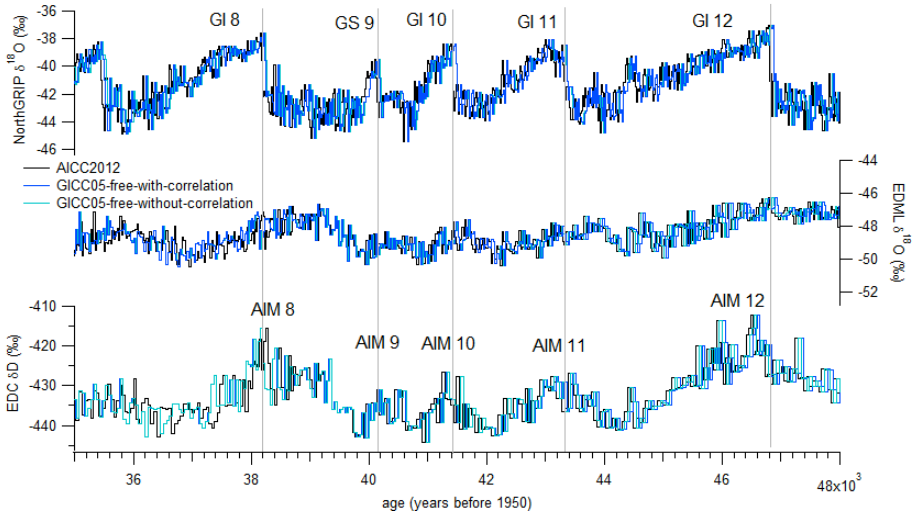

Figure 7. Comparison of NGRIP δ^{18}O (NorthGRIP Community Members, 2004), EDML δ^{18}O (EPICA Community Members, 2006, 2010) and EDC δD (Jouzel et al., 2007) water isotopes on different coherent chronologies (AICC2012 in black, GICC05-free with correlation in dark blue and GICC05-free without correlation in light blue).

CPD
10, 3585–3616, 2014